EXPERIMENTAL EVALUATION OF BATTERY CELLS
FOR SPACE-BASED RADAR APPLICATION

Craig A. Maskell

John R. Metcalfe

Defence Research Establishment Ottawa
Department of National Defence
3701 Carling Avenue
Ottawa, Ontario, K1A 0K2
Canada

Engineering and Quality Group
CAL Corporation
1050 Morrison Drive
Ottawa, Ontario, K2H 8K7
Canada

Abstract

A test program was conducted to characterize five space-quality nickel-hydrogen (NiH_2) battery cells. A subset of those tests was also done on five commercial nickel-cadmium (NiCd) cells, for correlation to the characteristics of an Energy Storage Unit Simulator. The test program implemented the recommendations of a 1991 study, as reported to IECEC-92. The findings of the tests are summarized, and expected impacts on the performance of the electrical power system (EPS) of a large space-based radar (SBR) surveillance satellite are derived. The main characteristics examined and compared were terminal voltage (average and transient) and capacity through discharge, equivalent series resistance, derived inductance and capacitance, charge return efficiency and inter-pulse charge effectiveness.

Introduction

Space-based radar needs a pulsed waveform and high power to detect targets, at long ranges against earth clutter. Many of the potential mission and radar profiles impose stringent requirements on the satellite's EPS. In many proposed concepts, for example, the radar coverage does not allow a sun-synchronous orbit, so the solar array must be augmented by a large battery. In addition, studies have shown that it is most efficient to supply most of the energy used by the radar from a battery — even during sunlit operation. Such SBR EPS concepts generally have battery charge/discharge pulse periods of 5-50 ms at duty cycles of 50% [1][2].

This SBR EPS concept configures up to 12 identical but independent sections, called power module strings, each to draw power from its own section of the solar array, contain its own battery and conditioning equipment, and feed a portion of the radar antenna. The batteries feed all loads during eclipse and provide about 70% of the radar power during sunlight. The solar array provides power to charge the battery between transmit bursts and when the radar is off. A module string battery is connected directly to the unregulated main transmission bus, with a nominal voltage of 120 V dc.

The discharge rate will be as high as 3C during radar transmit bursts. There may be up to a 0.8C charge rate available between those bursts. Assurance of good transient regulation of the bus is a major concern. Under such conditions, regulation is greatly influenced by the effective series resistance (ESR) and ac impedance characteristics of a 100-cell battery.

Terminal voltage (both average and transient) and capacity during discharge are important considerations. ESR, ac impedance characteristics, and charge return efficiency are parameters in predicting such performance factors.

NiH_2 battery cells are prime candidates for a first-generation SBR. In particular, NiH_2 cells have been demonstrated to have long cycle life at favorable depths-of-discharge. However, a study published in early 1992 revealed that their characteristics under the envisaged pulsed-loading were virtually unknown [1]. Until then, test programs generally looked at the performance, electrical characteristics, or life-cycle prediction under dc conditions. During the last year or so, however, some pulsed-mode tests have been done [3][4]. At least one cell manufacturer (Eagle-Picher Industries, Inc.) has also done some similar testing. Our test program extends this fledgling information base, with the parameters of the SBR EPS configuration in mind [1]. The results confirm that some of the critical performance variables of the cell, and consequently the battery, are markedly affected by this type of operation.

Our experimental evaluation had the following objectives:
- Determine various electrical characteristics of NiH_2 cells under representative pulsed-loading.
- Quantify the NiH_2 cell type's charge return efficiency and cell effective capacity.
- Detect anomalies or signs of NiH_2 cell degradation, but without cycle life testing.
- Compare the characteristics of the NiH_2 cells to commercial-type NiCd cells of similar capacity, to facilitate correlations with the Energy Storage Unit of a ground-based demonstration system.
- Predict EPS performance impacts of findings.

Table 1 — Description of the two types of battery cells tested under the evaluation program.

Cell Type	NiH$_2$	NiCd
Manufacturer	Eagle-Picher Industries, Inc.	SAFT Batteries Ltd.
Model No.	RNH 50-47 CAL	SHP 520
No. of Sample Cells	5	5
Rating (nameplate), Ah	50	52
Other features	• spaceflight quality • individual pressure vessel • 8.9 cm (3.5 inch) diameter; 1.5 kg • electrolyte concentration 27% KOH • positive (nickel) pre-charge • "rabbit-ear" terminal configuration	• commercial professional quality • electrolyte-flooded, vented • 8.5 x 8.5 x 27.0 x 26.4 cm • 3.6 kg • electrolyte: 20% KOH • single-ended terminal config.

Laboratory Set-Up

The test activities were carried out at CAL Corporation, Ottawa, Ontario. The NiH$_2$ and the NiCd cells (two series-connected strings tested consecutively) are described in Table 1. The installation centered on the facility's temperature control chamber — into which the test items on their fixture were placed. The facility included appropriate power connections, lighting, exhaust ducts and ventilation louvers. Provisions for safety and hazard control included a chamber hydrogen monitor and nitrogen purge equipment.
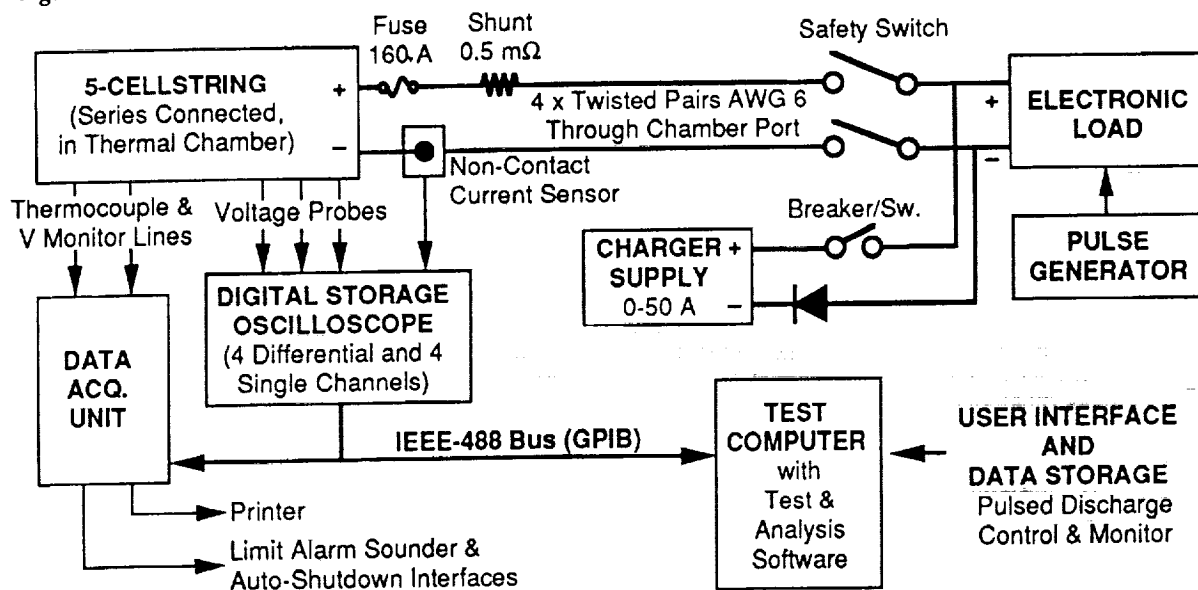
During all characterization cycles, the cell case temperatures were kept within ±2°C of the respective values specified for the NiH$_2$ and NiCd cells. For both cell types, auxiliary fans were placed to assist temperature regulation during high rate discharges.

To prevent unintentional electrical contact, the cases of the NiH$_2$ cells were conformally coated prior to installation in their heat-conductive mounting saddles.

Figure 1 shows the functional elements of the test system. The inter-pulse charging in some test cycles was accomplished by applying a constant current bias from the charger supply. The pulse generator drive level to the electronic load was set for the desired net cell current during the discharge pulses. This direct interconnection of the charger supply to the load and the test cell string resulted in some rounding of current transition edges due to regulating feedback loop, and output filter capacitance, of the charger supply. To get a response more representative of the intended application, at least for the load-off transition, a high-power schottky diode was installed in series with the supply's output.

Fig. 1 — Overview of the main functional elements of the battery cell test system.

Test Procedures and Analysis Methods

The NiH$_2$ cell characteristics were influenced by the following test parameters:

- Discharge Rate - pulsed (1-3C rates) & dc (1C and 2.5C rates) conditions
- Charge Rate - dc conditions only (at 0.5C and 0.8C rates, with step-down)
- Pulse Length (5, 20 & 40 ms "half-cycle")
- Current Rise/Fall Time (0.2-1.5 ms)
- Inter-Pulse Charge Rate (0.3-1.0C rates)

The NiCd cells were subjected to a limited subset of the parameters. The nominal test temperatures were restricted to 0°C for the NiH$_2$ cells and 10°C for the NiCd cells. Other cell types, and pulsed-mode life testing, were not explored. To further limit the number of test steps, the effects of changing only one variable at a time were tested, for a fixed set of the other variables.

A step-down in the charge rate was implemented during recharge of the cells. This was found necessary to limit cell voltage to a "safe maximum", and to provide an assessment point for consistency of cycle-to-cycle voltage versus state-of-charge (SoC).

SEQUENCE OF TESTS — Testing was done in 1992/93 in the following phases:

a. Initialization cycles of the NiH$_2$ cells; for re-activation and for comparison of reference capacity with that measured in acceptance testing.

b. Non-pulsed ("dc") characterization cycles of the NiH$_2$ cells; with combinations of 0.5C or 0.8C initial charge rates and 1C or 2.5C discharge rates through 1.0 V per cell.

c. Pulsed-discharge characterizations of NiH$_2$ cells; one load pulse amplitude, for three values of half-cycle time (load pulse width), versus two values of recharge rate, with and without inter-pulse charging.

d. Pulsed-discharge characterizations of the NiH$_2$ cells; one value of half-cycle time, for three values of load pulse amplitude, versus two values of recharge rate, with and without inter-pulse charging.

e. Pulsed-discharge characterizations of the NiH$_2$ cells; one value of half-cycle time and one of load pulse amplitude, versus four values of load current transition time, with and without inter-pulse charging.

f. Pulsed-discharge characterizations of the NiH$_2$ cells; one value of half-cycle time and one of load pulse amplitude, versus two values of inter-pulse charge rate.

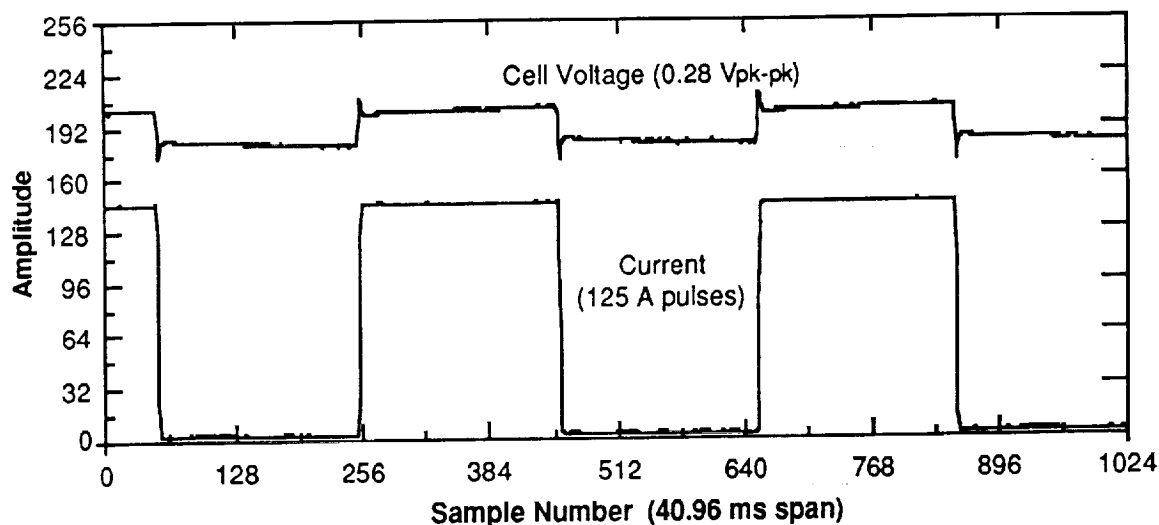g. Pulsed-mode and non-pulsed-mode capacity checks of the NiH$_2$ cells.

h. Activation cycles of the NiCd cells ; low-rate, non-pulsed.

i. Non-pulsed ("dc") characterization cycles of the NiCd cells; with 0.5C initial charge rate and 2.5C discharge rate through 1.0 V per cell.

j. Pulsed discharge characterization cycles of NiCd cells; with the "standard parameter set" of charge rate, load pulse width, amplitude and current transition time, with and without inter-pulse charging.

k. Non-pulsed-mode capacity check of NiCd cells.

Fig. 2 — Depiction of typical pulsed-discharge record "snapshot".

DATA ACQUISITION & STORAGE —
During pulsed-discharges, periodic wave-form
"snapshots" from the digital storage oscilloscope
were stored as ASCII files on the hard disk of the
Test Computer, as shown in the example in Fig. 2.
After each day of testing the files were copied onto
floppy disks. These snapshots were formatted for
easy loading into spreadsheet and graphing programs.
Generally, two columns containing from 1024 to
5001 amplitude values of current and voltage,
respectively, were stored.

Each data file has a header containing the record
number and, the date, time, cell string current, cell
voltages and cell temperatures, as transferred from the
data acquisition unit just prior to capturing the
oscilloscope trace. Eight different record types were
stored, in sequence, for most discharges. The voltages
of all five cells, and the cell string, were recorded
individually with several combinations of resolution
of sample time and amplitude.

Non-pulsed data, such as from dc charging, was
hardcopy-printed at regular intervals.

DATA RESOLUTION EFFECTS — The
accuracy of the results was limited by test equipment
effects such as the electronic load's current regulation
behaviour, and the ability to reduce measurement data
during analysis. We improved our analysis tools to
improve the typical quantizing resolution from
7 mV / 100 µs to 3.5 mV / 10 µs. In determining
plateau currents and voltages, and in estimating cell
resistances, averaging and/or iterating techniques
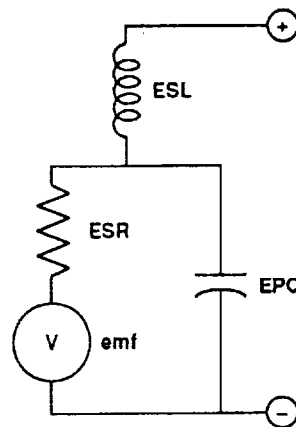further reduced granularity and improved accuracy.

ANALYSIS METHODS — Two main
methods were employed. The Observed Results
Method is suited for tabulation of larger quantities of
calculated voltages, currents and times, and the
resulting first-order approximations of effective series
resistance (ESR) and effective series inductance
(ESL). The Equivalent Model Method is an iterative
process which concentrates on a smaller number of
snapshot records to produce more accurate values of
the various impedance characteristics, including an
estimate of the capacitive component.

The two analysis methods are complementary.
For example, correction factors obtained from a few
runs of the Equivalent Model Method can be applied
to many values tabulated from the Observed Results
Method. All calculations were done on recent
versions of well-known spreadsheet programs.

EQUIVALENT MODEL ANALYSIS
METHOD — This method could be the subject of a
separate paper. (This is a cursory description only.)
The technique is intended to determine the values
applicable to an equivalent circuit model of the cell
under scrutiny.

We first postulated that the model would
consist of a voltage generator (electromotive force -
emf), a resistive element (ESR), and an inductive
element (ESL), all connected in series. During the
course of the analysis the necessity of including a
further element became clear. A capacitive element
(EPC) was thus added in parallel with the series
combination of emf and ESR, shown in Fig. 3.

Fig. 3 — Final equivalent circuit model of a cell.
The model does not include a possible second-order
capacitance in parallel with the circuit, being barely
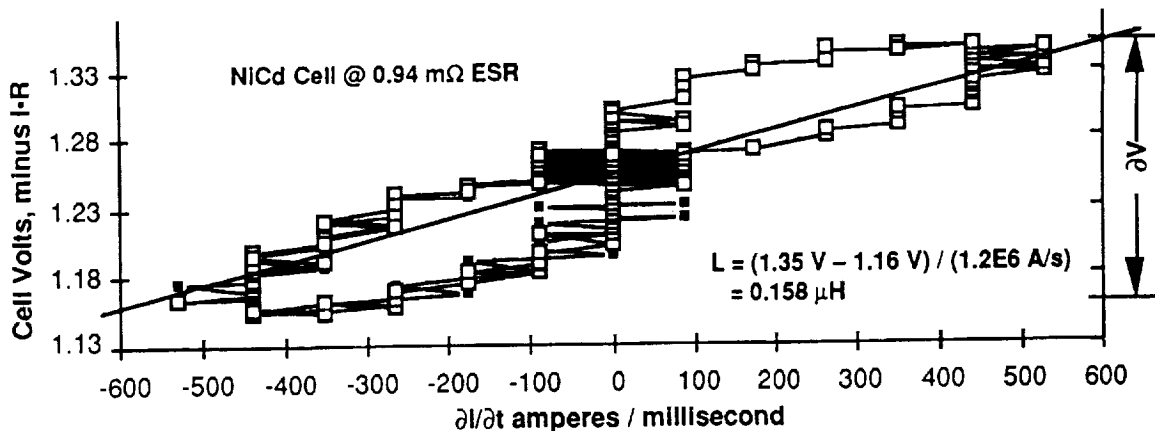detectable within the resolution of the data taken.

The values of ESR, ESL, EPC and emf can
only be considered as constants for the particular set
of conditions at the time the record was taken. By
determining values for these variables at various
spot-points of a pulsed discharge, it is possible to
relate their variations to SoC, and consequently to
interpolate the dynamic performance over the whole
discharge range.

The Equivalent Model Method evaluates the
elements one at a time and subtracts the effects of
that element from the original voltage vs. time data.
Typically, the value of the current multiplied by the
ESR is first subtracted to produce a new record
showing only emf and reactive-component voltage
effects. This reveals more clearly the effects of ESL
and enables its value to be estimated. Similarly, the
effect of inductance is then removed, enabling an
estimation of EPC.

After making any corrections necessary to time-
synchronize the current and voltage data columns, the
data values are converted to engineering units and
plotted one against the other. The best straight line
for the resistive component is visually estimated.
The variations from that line are the reactive
components of the cell.

The ESR estimate is multiplied by the current
of each sample point and the result subtracted from
the sample voltage. This yields the constant (emf)
component and the sum of the reactive components.

Fig. 4 — Example "eye" diagram for calculation of inductance.

The value of the inductance is then estimated from a plot of the $\partial I/\partial t$ value vs. the I*R product for each data sample (Fig. 4). The slope of the best straight line over the $\partial I/\partial t$ range then gives a ∂V value for use in computing inductance.

The time constant of the parallel RC circuit, resulting from the voltage generated across the ESR by the load current turning on and off, is then estimated. This involves a limited amount of averaging to filter the high frequency "noise" caused by the quantization levels of the digital storage oscilloscope. The decay is plotted. Dividing the time constant by the cell's ESR provides an estimate of the effective capacitance.

Cross-checking and result-refinement methods were also incorporated in the analysis. For example, the chart used to estimate the capacitance provided a sensitive tool for improving the resistance estimate. We could more accurately define the points where reactive effects have dissipated on the load-on and load-off pulsed-voltage profiles of the cell.

OBSERVED RESULTS ANALYSIS METHOD — This method assumes no equivalent circuit model for a cell, other than a series resistor for the ESR estimation and a series inductor for the inductance estimation. The "capacitive effect", as determined by the equivalent model method, is ignored for the ESR and L calculations here.

The Observed Results Method provides tables and plots to find overall voltage performance versus SoC (e.g., Fig. 5). It also provides rapid estimates of reactive components which can be correlated with the results of the equivalent model method.

The voltage plateaus (load-on and load-off) are defined here as the segments, in time, following observed recovery from the inductive spike and until just prior to the start of the next transition. The average voltage for each selected plateau period was computed. The ESR of the cell (for that part of the

discharge) is the ratio of the difference between two successive average plateau voltages to the difference between two corresponding average current plateaus (converted to A). The ESR by this method is an "apparent ESR" because it still contains some of the complex components of plateau impedance (Fig.7).

Voltage recovery from an inductive spike is arbitrarily defined as the point where the data values representing the cell voltage do not vary more than ±1 bit in amplitude over three samples (usually just two or three samples into the period of settled current on the record). The converse definition applies to define the end of a voltage plateau before a transition.

Results and Discussion

The analyses of pulse plateau voltage and cell resistance showed that the capacitive time constant of the cell decreases the apparent ESR of the cell for the shortest test load-pulse width (5 ms). Better ripple-voltage performance thus results from shorter pulses.

No performance degradation or malfunction of any kind was detected in the NiH_2 cells. This was confirmed by examining cell round-trip efficiency, discharge capacity and mid-discharge voltage tabulated over the course of the testing.

Following are observed trends, from the overall results, in values of equivalent circuit elements versus state-of-charge:

- emf decreases with decreasing SoC, sharply from full charge, for both NiH_2 & NiCd cells.
- ESR increases at lower SoCs, for both the NiH_2 and NiCd cells tested.
- Inductance appears to increase slightly at lower SoCs — NiH_2 cells.
- Inductance appears to decrease slightly at lower SoCs — NiCd cells.
- EPC decreases gradually with decreasing SoC, for both the NiH_2 & NiCd cells tested (Fig.6).

Fig. 5 — NiH$_2$ discharge voltage profile, pulsed-mode standard vs. dc-mode standard conditions — one of several plotted from test results of different load current levels. SoC is referenced to 1 V EODV defining 100% discharge.
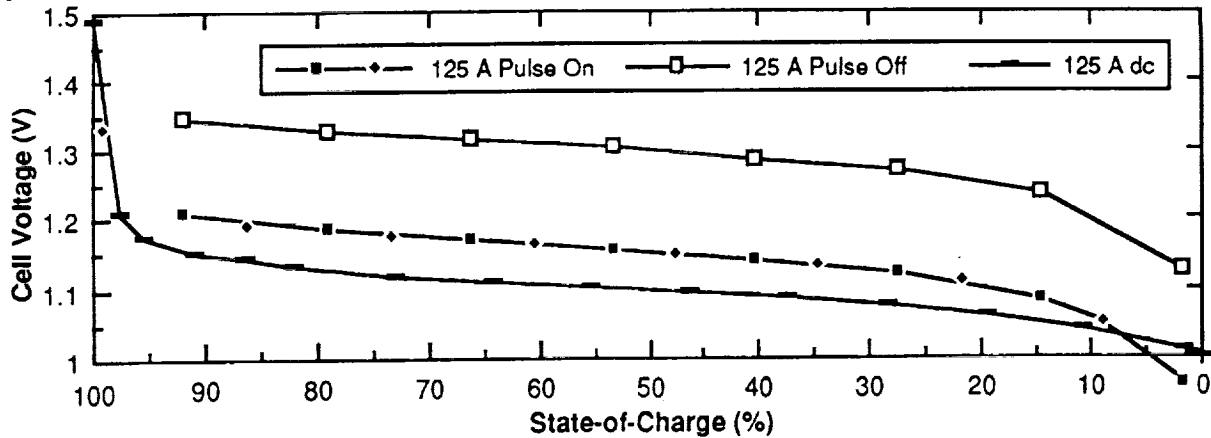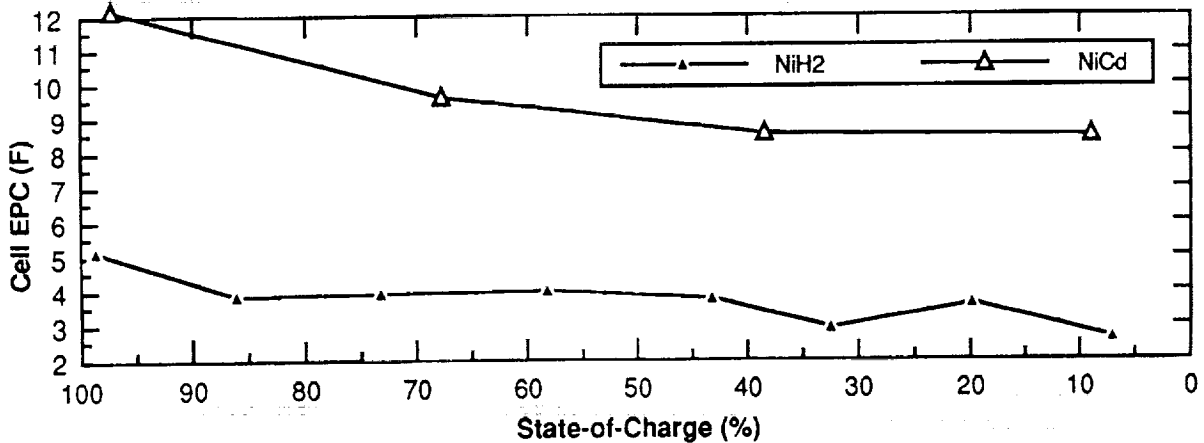

Fig. 6 — NiH$_2$ and NiCd cell capacitance vs. SoC results of Equivalent Model Method; standard test condition. SoC is referenced to 1 V EODV defining 100% discharge. Typical cell characteristics are listed in Table 3.

PERFORMANCE PREDICTIONS FOR FLIGHT NiH$_2$ BATTERY — The performance of an SBR battery may be predicted coarsely by extrapolating the transient characteristics of the five-cell test string. For example, under the "standard parameter regime" (2.5C rate pulses; 400 µs transitions), the typical 1.73 V peak-to-peak spike voltage envelope of the string extrapolates to 6.92 V for a 20-cell pack. With an allowance of 10% for inter-pack connections, this spike envelope would increase to 38 V for the five-pack (100-cell) battery envisaged for SBR. Computer P-Spice modelling

indicates that, should this be a problem, putting a moderate-size RC filter across the main bus interface of the Energy Storage Unit will sufficiently dampen spike amplitudes in the SBR EPS configuration [5].

Regulating the ripple between the two voltage plateaus then becomes the EPS performance trait influenced most directly by the cells' ESR and time-constant characteristics. A typical 0.75 V plateau-to-plateau ripple of the five-cell string under "standard parameters" (125 A load pulse, 20 ms half-cycle) can thus be similarly extrapolated to 16.7 V for the full-battery estimate.

Table 2 — Performance extrapolated to a 100-cell NiH$_2$ battery (five series-connected packs of 20 cells). The source values used for these estimates are for approximately 80% SoC and, except for emf and plateau voltage, were considered typical for the 60-100% SoC range.
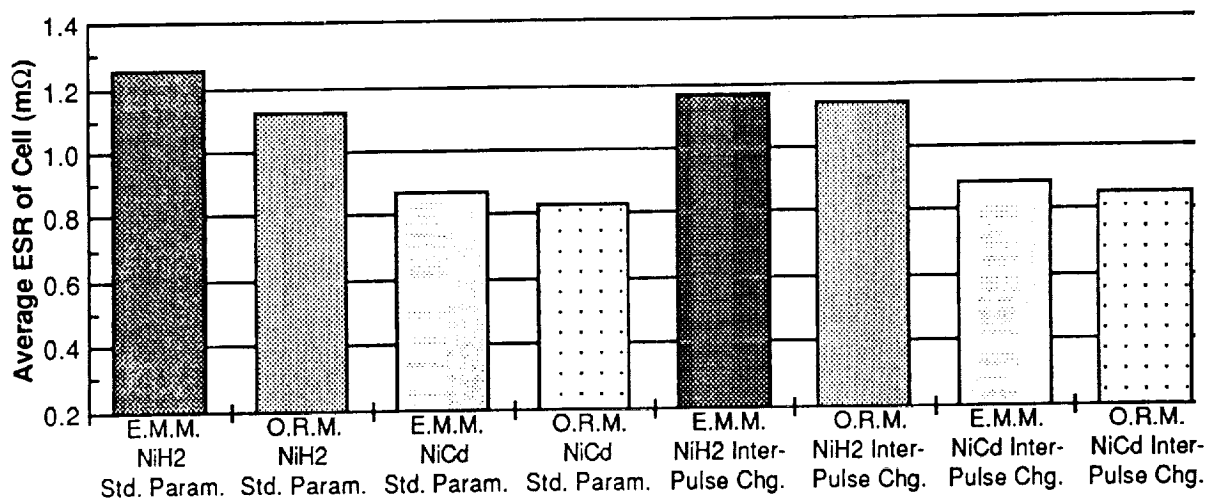
emf (V)	Plateau Avg. Load-Off (V)	Plateau Avg. Load-On (V)	Line Regulation (Ripple; V)	ESR (mΩ)	ESL (µH)	EPC (F)
133.8	132.5	115.8	16.7	151	15	0.04

Table 3 — The principal correlations between the NiH$_2$ and NiCd cell characteristics.

Variable	NiH$_2$ Cell	NiCd Cell	Notes
Voltage	1.47 V	1.38 V	Electromotive Force; 98% SoC with 125 A pulse amplitude
Voltage	1.32 V	1.27 V	Electromotive Force; 60% SoC with 125 A pulse amplitude
Capacity (dc 1)	55.8 Ah	32.3 Ah (24°C)*	Discharge to 1.0 V; avg. 50 A rate; non-pulsed
Capacity (dc 2)	46.8 Ah	21.0 Ah *	Discharge to 1.0 V; avg. 125 A rate; non-pulsed
Capacity (Pulse)	56.2 Ah	24.8 Ah *	Discharge to 1.0 V; avg. 125 A pulses (62.5 A avg.)
Round-Trip Efficiency	~92% (1C dc rate) ~80% (2.5C dc rate) ~89% (1C pulses) ~90% (2.5C pulses) ~89.5% (3C pulses)	inconclusive for NiCds (52.5-58% range in tests due to extended charges)	Typ. Round-Trip Capacity Efficiency; charge removed in discharge divided by previous charge I/P of same cycle. NiH$_2$ R-T.C. efficiencies slightly less (typ. 1%) w. inter-pulse charging & slightly more w. 0.8C rate charging.
Inter-Pulse Charge Eff.	~95%	~99% (inconclusive)	% of charge I/P seen as useful capacity at load (vs. std. disch.)
Static Resistance	1.52 mΩ	1.38 mΩ	R from ∂V/∂I for const. 125 A vs. 50 A disch. rates; 80% SoC
ESR	1.25 mΩ	0.87 mΩ	Equivalent Series Resistance (Avg. from 60-100% SoC)
ESL	~0.15 μH	~0.2 μH	Equivalent Series Inductance (Avg. from 60-100% SoC)
EPC	~4 F	~11 F	Equivalent Parallel Capacitance (Avg. from 60-100% SoC)

* Nameplate capacity defined by *low-rate* discharge in commercial cells.

Fig. 7 — Comparison of the NiH$_2$ and NiCd ESR results from the two analysis methods — the Equivalent Model Method (E.M.M.) and the Observed Results Method (O.R.M.). The static resistance of the NiH$_2$ cell (measured by comparing voltages at different dc discharge currents) is about 25% greater than its ESR (based on pulsed waveform voltage and current analysis). For the NiCd cell model tested, the static resistance is about 50% greater than the ESR.

By the same reckoning, an improvement to about 15 V of ripple can be predicted from the 5 ms half-cycle-time results.

Some of characteristics in Table 2 are also dependent on other battery variables. For example, the 151 mΩ ESR estimate may be reduced, perhaps by more than 10%, by use of ultra-low-resistance cell and cell-pack interconnection techniques.

Recommendations

The NiH$_2$ cells tested are well-suited to this type of pulsed-load application. However, they are slightly higher in equivalent series resistance than desired. For such a high-current application, this might be improved by having larger connection terminals to lower the contact and feed-through resistances. This possibility should be investigated, but any modification should not change the basic cell design, nor significantly impact specific energy. Another possible way to decrease cell resistance is to consider cells of higher capacity ratings, e.g., having more electrodes, but of the same basic design.

In the near term, cells of the design variant tested here are virtually ideal for an SBR-type application. However, common pressure vessel technology is maturing rapidly. For example, two-cell modules have been accumulating impressive life-cycle numbers. In the longer term, such mass and energy saving modules should be considered for the SBR application, and pulsed-modes characterization testing should be done.

The test program has unveiled questions regarding cell and battery performance and its impact on performance of the SBR EPS. For example, the effects of pulsed-discharge and inter-pulse charge conditions on cycle life of a cell are not known: Does inter-pulse charge accelerate capacity degradation because each pulse cycle resembles a very low-depth charge/discharge cycle? A long-term cycle life test would answer that question.

Conclusions

NiH$_2$ cells of the type tested should provide good performance in the envisaged SBR EPS. No operational anomalies were observed and performance variables such as discharge capacity were consistent. Use of the 27% KOH electrolyte concentration and of the nickel pre-charge process did not adversely affect suitability of the cycle voltage profile nor of any other traits examined.

The goal of an operational pulsed-mode battery resistance of less than 150 mΩ, with acceptable amplitudes of bus voltage swing, is achievable with the NiH$_2$ cells tested. For the Energy Storage Unit Demonstrator, also containing 100 cells — but of the commercial NiCd model, an operational

resistance of about 80 mΩ has been achieved due to lower cell ESR and low interconnection resistances.

An apparently capacitive time constant, which can improve bus voltage regulation at faster radar burst repetition rates, has been identified and quantified. Voltage ripple between the load-on and load-off plateaus of a NiH$_2$ cell is less for a half-cycle time briefer than the "capacitive" time constant (i.e., the characterized 5 ms period vs. 20 ms and 40 ms periods).

The transient voltage spikes are greater at higher pulsed current rates and with faster current pulse transition times, due largely to the ESL of the cells. For all of the pulsed parameter combinations tested, these spikes will be readily manageable by capacitive filtering on the main power bus.

The fact that pulsed-mode ESR is substantially lower than static cell resistance indicates that a large improvement in cell efficiency can be expected in the pulsed mode of operation over the normal dc mode. The operation should be restricted to the higher states-of-charge, as is usual.

Charging between radar transmit bursts is reasonably efficient under the tested parameters. Charge and discharge round-trip efficiency is reduced at high inter-pulse charge current rates.

Charge and discharge round-trip efficiencies were found to be much less affected by the amplitude of the discharge current in pulsed mode than in dc mode.

The impedance characteristics of the NiCd test cells have been shown to be similar to those of the NiH$_2$ cells. This commercial type of NiCd should thus be satisfactory for use in the energy storage demonstration unit.

The data provides an abundance of information on the cells' dynamic electrical characteristics.

Acknowledgements

References

1. Maskell, C.A.; Metcalfe, J.R. *Proc. 27th IECEC*, 1992, pp 1.153-1.157.
2. Maskell, C.A. *Proc. 26th IECEC*, 1991, pp 1.340-1.345
3. Capulli, J.; Myers R.; Murray, I.; Lurie, C.; Johnson, E.W.; Griebel, R. *Proc. 27th IECEC*, 1992, pp 1.511-1.519.
4. Hafen, D. *Proc. 27th IECEC*, 1992, pp 2.99-2.104.
5. Tanju, M.C. Proc. *European Space Power Conference*, 1993, pp 1.87-1.92.